Published in final edited form as:
ACS Nano. 2018 February 27; 12(2): 1482–1490. doi:10.1021/acsnano.7b07983.

Proteolytic nanoparticles replace a surgical blade by controllably remodeling the oral connective tissue

Assaf Zinger[1], **Omer Adir**[1], **Matan Alper**[1], **Chen Tzror**[1], **Assaf Simon**[1], **Shira Kasten**[1], **Zvi Yaari**[1], **Maria Poley**[1], **Janna Shainsky-Roitman**[1], **Sharon Akrish**[2], **Tidhar Klein**[3], **Dov Hershkovitz**[4], **Avi Schroeder**[1,*]

[1]Department of Chemical Engineering, Technion – Israel Institute of Technology, Haifa 32000, Israel

[2]Department of Oral and Maxillofacial Surgery, Rambam Medical Center, Haifa, Israel

[3]Moriah Animal Companion Center, Haifa, Israel

[4]Department of Pathology, Tel Aviv Sourasky Medical Center, Israel

Abstract

Surgical blades are common medical tools. However, blades cannot distinguish between healthy and diseased tissue, thereby creating unnecessary damage, lengthening recovery and increasing pain. We propose that surgical procedures can rely on natural tissue remodeling tools – enzymes, which are the same tools our body uses to repair itself. Through a combination of nanotechnology and a controllably activated proteolytic enzyme we performed a targeted surgical task in the oral cavity. More specifically, we engineered nanoparticles that contain collagenase in a deactivated form. Once placed at the surgical site collagenase was released at a therapeutic concentration and activated by calcium, its biological cofactor that is naturally present in the tissue. Enhanced periodontal remodeling was recorded due to enzymatic cleavage of the supracrestal collagen fibers that connect the teeth to the underlying bone. When positioned in their new orientation, natural tissue repair mechanisms supported soft and hard tissue recovery and reduced tooth relapse. Through the combination of nanotechnology and proteolytic enzymes, localized surgical procedures can now be less invasive.

Keywords

nanotechnology; protein delivery; bio-surgery; extracellular matrix

Five-million patients undergo orthodontic procedures annually in the US alone[1]. In cases of severe malocclusion a minor surgical intervention is necessary in order to maneuver the teeth to their proper position (Figure 1A)[2]. During this procedure collagen fibers that connect the teeth to the underlying alveolar bone are sectioned with a scalpel (Figure 1B). After the surgery, braces are used to maneuver the teeth to their proper orientation. Despite the potential benefits of surgery, many patients opt not to undergo such procedures due to

* avids@technion.ac.il.

Europe PMC Funders Author Manuscripts

their invasive nature. Here, we tested the ability of nanoparticles loaded with a proteolytic enzyme to replace such procedures by directly targeting collagen type-I fibers in the oral cavity (Figure 1C).

There are 28 types of collagens in the human body that are tuned for the mechanoelastic function of each organ. In the oral space (specifically in the gingiva), collagen type-I supra-crestal fibers connect between the teeth and the alveolar bone. During orthodontic procedures, tooth movement depends on remodeling of the supra-crestal collagen fibers and bone[3]. This force-induced process can be painful[4], and, for its successful completion, requires that the collagen fibers remodel in line with the final positioning[5].

Collagenase is a matrix metalloproteinase which is naturally in control of biodegrading collagen in the extracellular matrix[6] and a key player in tissue remodeling processes[7]. Collagenase is clinically-approved for digesting abnormal thickening of the skin and tissues of the palms in patients suffering from Dupuytren's contracture[8]. In order to prevent damage to collagen-containing tissues that surround the treatment site, the enzyme concentration and spatial biodistribution must be carefully controlled.

Nanotechnologies promise to revolutionize medical care by[9] improving accuracy and targeting therapeutics to the disease site[10–11]. To date, more than 80 nanotechnologies have been approved for clinical use[12–13]. Liposomes, nanoscale vesicles with an inner aqueous core that is surrounded by a lipid bilayer membrane, are clinical drug delivery systems[14]. Tailoring the liposome size and composition modulates biodistribution and controls the drug release profile at the target site[15]. For example, liposomes are used for targeting anticancer agents to tumors or for the localized controlled-release of analgesics. However, the delivery of enzymes from liposomes remains a challenge[16].

In this study, we developed a drug delivery system that releases the proteolytic enzyme collagenase type-I to remodel collagen-I fibers in the oral space, to replace a minimal surgery performed in the oral space.

Results

Collagenase nanoparticles inhibit early activation of the enzyme

Collagenase is a proteolytic enzyme that cleaves the collagen backbone by detaching the peptide bond between glycine and leucine or isoleucine[17]. We chose to work with collagenase type-I to relax the supra-crestal collagen-I fibers that connect the teeth to the underlying alveolar bone.

Collagenase is activated by calcium, its biological cofactor, which catalyzes the proper folding of the enzyme and enables collagenase binding to its collagen substrate (Figure 1D). Once activated, the half-life of collagenase is several hours until it is retarded by metalloproteinase inhibitors or by other physiological conditions (Figure 1E). We sought to develop a system in which collagenase is activated only after it is placed at the surgical site. For this, we loaded collagenase into the 100-nm liposomes in the absence of Ca. The liposomal lipid bilayer, composed of 1,2-dimyristoyl-*sn*-glycero-3-phosphocholine **(**DMPC),

is impermeable to Ca^{2+} ions (Figure 1E)[18]. This impermeability protects the enzyme from early activation (Figure 1D, E). The liposome lipids were not susceptible to degradation by collagenase (Supplementary Fig. S1). Once placed in the sulcus, collagenase began diffusing out of the liposomes (Figure 1F). Naturally present in the oral cavity, the calcium activated the enzyme, which in turn began relaxing the collagen fibers (Figure 1G,H).

Collagenase relaxes collagen fibers in a concentration-dependent manner[19]

More than 300 collagen fibers were stressed in the presence of collagenase at different concentrations using an experimental setup that mimics the physiological conditions (Figure 1G). The tensile strength of each collagen fiber was measured as a function of the collagenase concentration and treatment time.

As the concentration of collagenase increased the fibers weakened (Figure 1H). During this process, a therapeutic collagenase concentration of 0.05-0.1 mg/mL was determined, at which the fibers relaxed but did not tear. We expressed the relative change in fiber strength during the treatment using a dimensionless number, α:

$$\alpha = \frac{Force\ needed\ to\ tear\ a\ collagenase\ treated\ fiber}{Force\ needed\ to\ tear\ an\ untreated\ fiber}$$

A descending α slope implies that the collagen bundle is weakening, while an ascending slope implies that a reparative process is occurring. Three modes of α can be noticed, as the collagen bundles are being exposed to collagenase (Figure 1H, Supplementary Fig. S2). At first, rapid weakening of the fibers treated with collagenase was recorded ($0<\alpha<0.2$). Thereafter, some strengthening of the collagen fibers occurred ($0.2<\alpha<0.4$) followed by gradual collagen weakening until the fiber tore ($\alpha=0$). The weakening of the collagen is intuitive due to the degradative activity of the collagenase. However, the strengthening of the fiber suggested that endogenous collagen repair mechanisms are activated after the fiber is exposed to collagenase.

Fibroblasts remain adherent to the collagen fiber throughout the treatment, secreting remodeling factors and initiating collagen repair[20]

Fibroblasts play an important role in collagen remodeling[21]. Adherent to the collagen fibers, fibroblasts sense the fiber tension and initiate regenerative processes when the fiber is degraded. Using a time-lapse laser scanning confocal microscopy, we imaged the fibroblast morphology in response to the collagenase treatment (Figure I-K). When the fiber was stretched, the fibroblasts had an elongated, ellipse morphology (Figure I). Due to the exposure to collagenase, the fiber relaxed and the fibroblasts assumed a round structure (Figure 1J,K; a time-lapse movie of the morphological change in the adherent fibroblasts: https://youtu.be/4krwecUS7Yc). Interestingly, throughout the process we did not observe fibroblast detachment from the fiber and fibroblast viability was retained (Figure 1I-K). This finding suggests that natural reparative processes can be carried out by the adherent fibroblasts (Figure 2).

Collagen regeneration

Using collagen type-1 fibers sourced from a rat, we were able to observe the regenerative process after the enzymatic treatment (Figure 2A-C). The mechanical properties of the collagen fibers were tested before, during and after the exposure to collagenase (Figure 2D). The tensile strength of the collagen fibers was approx. 5 N before being exposed to collagenase. After exposing the fibers to a therapeutic dose of collagenase, their strength decreased by approximately 50%. As expected, 16 hours after completing the process, the fibers regained their initial strength (Figure 2D).

Throughout the treatment we imaged the morphological changes that the collagen fiber undergoes using scanning electron microscopy (Figure 2A-C). Before the treatment we observed that the collagen has a tightly packed fiber structure. After being treated with collagenase, the collagen fibers unraveled (Figure 2A). Several hours after retarding the collagenase activity, collagen fibers resumed their initial morphology (Figure 2B) with the exception of some regions of the regenerated fiber which were not perfectly aligned (Figure 2C). There is a slight discrepancy between the time it takes the fiber to reach visual repair (as seen under the electron microscope) and mechanical repair (as measured using a force machine). Even though the fiber appears regenerated, the internal molecular bonds between the collagen bundles may require more time to fully develop.

Collagen-repairing genes are activated following the procedure

Regenerative biological cascades were triggered in response to the degradative signal. We applied collagenase type-1 to rat's gingiva, *in vivo*. Twenty-four hours later the tissue surrounding the teeth was collected and RNA was isolated. The RNA profile of genes that are associated with collagen repair and extracellular matrix remodeling was measured (Figure 2E). We found that multiple genes were upregulated in the treated tissue; namely, Col-1a1, a gene that encodes for collagen type-1 synthesis, IL1B, a gene that is associated with osteoclast activation and TNC, a gene that is expressed during remodeling of the extracellular matrix (Figure 2E).

Enzymatic nano-surgery versus surgery with a scalpel

We compared the efficacy of rats treated by nanoparticulate enzymatic surgery to rats that underwent traditional surgery with a scalpel. Collagenase-loaded liposomes were inserted into the gingival sulcus, and tooth alignment was evaluated using an orthodontic spring (Figure 1A-C).

Over a treatment period of 15 days, we measured a similar enhancement of the tooth alignment trajectory motion in rats that underwent a surgical procedure in which the supra-crestal collagen fibers were sectioned with a scalpel, and in rats that underwent the nano-enzymatic procedure (Figure 3A-C). The nanoparticulate collagenase group had enhanced tooth alignment compared to both the sham group (empty liposomes) and the group treated with the free enzyme (Figure 3D). The liposomal nanoparticulate collagenase group also displayed a three-fold enhancement in tooth alignment compared to ordinary braces (Figure 3D). The accelerated tooth movement in the nano-surgery group compared to the other treatment groups is attributed to the biological relaxation of the collagen fibers. After 15

days, the teeth reached their maximal magnitude of mobility and the orthodontic spring was removed. The improved in vivo activity of the nanoparticulate delivery system corroborates the rapid in vitro deactivation of the free enzyme (Figure 1E). This suggests that the liposomal systems protected the enzyme in vivo, prolonging its release profile and confined the spatial distribution of the enzyme to the treatment site (Figure 3E). The delivery system prevented the enzyme from deactivating prematurely and allowed it to maintain its therapeutic activity as compared to the free enzyme group.

Localized biodistribution of the enzymatic nano-surgery liposomes

One requirement a nano-surgery system must satisfy is specificity to the target site. This is achieved by selecting the proper proteolytic enzyme tailored biologically towards the target organ. In addition, the drug delivery system must confine the spatial biodistribution of the enzyme primarily to the treatment site and maintain the therapeutic dose needed for the surgery. To confine the release of collagenase to the treatment site, we tested the biodistribution of liposomes (100 nm) loaded with a florescent dye after being placed in the sulcus (Figure 3E). The nanoparticles remained in close vicinity of the treated tooth for 24 hours. Eight hours post administration, we found traces of the particles also around the tongue due to liposomes leakage from the sulcus but not in the liver, heart, kidneys or spleen (Figure 3E). Histological evaluation of these tissues demonstrated that they were unharmed (Figure 3F-O), most likely due to the collagenase deactivation in saliva (Figure 1E).

Aseptic inflammatory processes play a major role in preconditioning the alveolar bone for orthodontic tooth movement[22]. We compared the degree of inflammation in rats treated with ordinary orthodontics to those with orthodontics supplemented with non-encapsulated collagenase, liposomal collagenase and surgery. Histological analysis of the gingival tissue shows similar presentation of mild inflammation among all groups (Figure 3F-O, Supplementary Fig. S3).

Interestingly, the animals' eating patter was minimally affected by the treatment. During the first week all rats lost ~10% of their body weight. A similar weight-loss profile occurs also in humans undergoing orthodontic treatments and is associated with adapting to a device in one's mouth. After completing the treatment, only the nanoparticulate enzymatic rats regained the weight they lost (Supplementary Fig. S4). In comparison, rats treated by the traditional surgery displayed weight loss. Even though the teeth moved three-fold greater distance in the nano-surgery group, the rats continued eating solid pellet chow and regained normal weight, suggesting this treatment approach is associated with less discomfort.

Tissue remodeling after nano-surgery

Regeneration of the soft and hard tissues that surround the teeth is necessary after a surgical process. We observed the changes the alveolar bone underwent throughout the enzymatic process. For this, microCT scans of the maxillofacial bone were performed 15 days after initiating the treatment and 45 days after removing the braces (i.e. day 60 of the experiment, Figure 3P-S). Interestingly, bone recovery was faster and to a greater extent in the nano-enzymatic group compared to bone repair in the group treated with ordinary braces. At the beginning of the procedure, in tandem with tooth movement, bone absorption was observed

Europe PMC Funders Author Manuscripts

at the treatment site (Figure 3Q). On day 60 (45 days after removing the braces), full bone recovery was observed at the new tooth orientation (Figure 3S). These findings suggest that the periodontal bone regenerates in an improved manner after the nano-enzymatic surgical procedure.

Enzymatic nano-surgery reduces tooth relapse

Relapse is a condition in which the teeth shift out of alignment back to their pre-orthodontic treatment position. Approximately 40% of patients suffer relapse, usually leading to a second cycle of orthodontic treatment[23]. To avoid relapse, dentists affix the teeth using NiTi wires. Interestingly we noticed that nano-surgery treated rats had significantly less tooth relapse in comparison to the control group (Figure 3H). On day sixteen after removing the braces the regular treatment completely relapsed, while the enzymatic nanoparticle treatment retained a held a 1 mm displacement gap at the treatment site. (Supplementary Fig. S5) We attribute the slow relapse in the nanoparticle treated group to improved regeneration of the collagen fibers and bone at the target position.

Discussion

Orthodontic procedures are prevalent among teenagers and adults. In many cases a surgical intervention is necessary in order to maneuver the teeth to their proper position with braces.

Our goal was to develop a new mode for performing biological, rather than physical, remodeling of connective tissue in the oral space. We demonstrate that controlled delivery of proteolytic enzymes using nanotechnology can replace minimal surgery.

Collagenase, a proteolytic enzyme with specificity towards collagen, plays a major role in remodeling the extracellular tissue matrix. Due to its degradative nature, collagenase has a short half-life and working distance *in vivo*, mitigating its effect only to its substrate[24]. Here, we harnessed collagenase, by integrating the enzyme into a drug delivery system, to degrade the supra-crestal in a controlled manner. Specifically, liposomes, vesicles with an inner aqueous core surrounded by a lipid bilayer, were loaded with collagenase and applied to collagen fibers. At a therapeutic collagenase concentration of 0.05-0.16 mg/mL the fibers relaxed but did not tear. The enzymatic treatment did not detach adherent fibroblasts from the collagen fibers. Moreover, secreted biomarkers indicated that the collagen was repaired by the fibroblasts. The repair was confirmed by the regeneration of the tensile strength and morphology of the collagen fibers over time.

When placed in the sulcus of rats (between the gingival tissue and the tooth) collagenase facilitated enhanced orthodontic tooth movement at three times the rate of ordinary braces. Histological sections of the treatment site demonstrated minor inflammation following the treatment. During the treatment the animals did not lose weight, suggesting that despite the enhanced tooth motion the animals did not suffer increased oral pain that would prevent them from access to chow.

Relapse, the return of teeth to their pre-treatment orientation, is a major challenge in orthodontics. Reduced tooth relapse was observed after the braces were removed in the

enzymatically-treated group. This is attributed to soft and hard tissue remodeling at the new orientation rather than the return of the stressed teeth to their original orientation in the control group. CT scans during the therapeutic process and 45 days following the braces removal indicated that the underlying bone remodeled in the new orientation. Compared to traditional surgery, the enzymatic treatment achieved an improved outcome, had better recovery and suggests less pain.

In summary, this study provides a new approach for degrading connective tissue using proteolytic enzymes housed in nanoparticles rather than by surgical intervention. Combining nanotechnology and enzymatic drug delivery may prove effective in treating conditions where a tissue must be remodeled in a specific manner. This non-invasive procedure was shown to shorten the treatment time and improve recovery.

Materials and Methods

Liposome preparation

Collagenase type-1 was incorporated into 100-nm liposomes. A lipid mixture of 1,2-dimyristoyl-sn-glycero-3-phosphocholine (DMPC; Avanti Polar Lipids, Alabaster, Alabama), cholesterol (Sigma) and 1,2-distearoyl-sn-glycero-3-phosphoethanolamine-N-methoxy-polyethylene glycol 2000 (Avanti) in a molar ratio 56:39:5 was dissolved in 200 ml 70% ethanol. The mixture was subsequently hydrated in Dulbecco's Phosphate Buffer Saline containing the collagenase (DPBS, Sigma-Aldrich, St. Louis, USA) to reach a lipid concentration of 50 mM. The liposome dispersion was extruded at 45 °C using a high-pressure Lipex extruder (Northern Lipids, Vancouver, Canada) and sequential passaging through Nuclepore polycarbonate membrane membranes (Whatman, Newton, MA, USA) with a pore diameter of 800, 400, 200, and 100-nm. Five extrusion steps were applied per filter type. The average diameter size of the liposome's distribution was determined by dynamic light scattering (DLS) using Zetasizer Nano ZSP (Malvern Instruments, UK). The mean size of the liposomes was 110-130 nm with polydispersity index (PDI) of 0.04-0.09. The liposome solution was then dialyzed against a phosphate buffered saline solution for 24 hours, exchanging the external media after 1, 3 and 24 hours.

The encapsulation fraction of the collagenase was measured using microBCA assay following the dialysis process. The liposomes entrapped 8-10% of the initial amount of collagenase in the solution ~160-200 ug/ml, i.e., 0.14-0.18 mg/ml in the liposomal dispersion.

To load the enzyme without compromising its activity, a maximal working temperature of 50°C, extrusion pressure of 10 bar, and ethanol content below 10% v/v was used (Supplementary Fig. S6).

Particle' biodistribution

Biodistribution experiment was performed on male Wistar rats using the Maestro *in-vivo* imaging machine (Cambridge Research & Instrumentation, MA, USA) calibrated to the following parameters: system wavelength: 780-820, exposure: 5000, excitation filter: 690 nm, emission filter: 750 nm.

ICG (indocyanin green) was encapsulated in multi-lamellar liposomes dissolving 1,2-dimyristoyl-sn-glycero-3-phosphocholine (DMPC, Avanti Polar Lipids, Alabaster, Alabama) and cholesterol (Sigma-Aldrich, St. Louis, USA), 70:30 mole ratio in ethanol. The lipid mixture was applied into phosphate buffered saline containing 1.8 mg/ml ICG, to form florescence multi-lamellar liposomes. To produce unilamellar liposomes the solution was extruded at 45 °C using a high-pressure Lipex extruder (Northern Lipids, Vancouver, Canada) and sequential passaging through Nuclepore polycarbonate membrane membranes (Whatman, Newton, MA, USA) with a pore diameter of 800, 400, 200, and 100-nm. Five extrusion steps were applied per filter type. The solution of florescent multi-lamellar liposomes was dialyzed with PBS overnight in order to separate the encapsulated ICG from the non-encapsulated one.

The florescent multi-lamellar liposomes were simultaneously applied to 5 male Wistar rats on each side of the 1st upper molar, 100 μl to each side. These were the same delivery sites used for the efficacy experiment.

The total length of the experiment was 24 hours, in which measurements were taken in the following times: 0, 1, 4, 8, 12, 24-hr.

For every measurement, the rat was dissected, and the organs were tested using the CRI Maestro *in-vivo* imaging machine.

The result's intensity values were normalized to the highest signal in all organs. Values under 0.5% of the highest value were neglected.

Thin Layer Chromatography (TLC)

Liposomes were synthesized and split into two groups: empty liposomes and collagenase encapsulated. Liposomes were dissolved in a Tris-buffer with Ca^{+2} ions. All groups were loaded onto a silica-gel TLC plate and then placed into a TLC chamber with the mobile phase a chloroform-methanol-water solution (65:25:4). The plate was held until the mobile phase reached a critical height, versus all 4 of their components separately: collagenase, cholesterol, PEG-2000 and DMPC.

Collagenase activity assay

Collagenase activity was assessed using fluorescein conjugated gelatin (Thermo Fisher) as a substrate. The enzyme solution was added to the substrate solution together with a reaction buffer (0.5 M Tris-HCl, 1.5 M NaCl, 50 mM $CaCl_2$, 2 mM sodium azide, pH 7.6). Fluorescence intensity for every sample was measured every 15 seconds for 3 minutes with excitation set at 485 nm and emission at 530 nm using the Infinite 200 PRO multimode reader (TECAN, Mannedorf, Switzerland). A linear incline was determined, and collagenase concentration was calculated using a calibration curve generated by collagenase samples of known concentrations.

Collagenase release assay

Collagenase release was assessed using a Micro BCA Protein Assay Kit (Thermo Fisher Scientific, MA, USA). To separate between the encapsulated and released collagenase, the

liposomal solutions that were incubated for each of the experimental time points (1-50 hrs) were ultra-centrifuged for 45 minutes with the following parameters: 4 °C, 45,000 RPM. After the centrifugation the supernatants were incubated with Triton X-100 diluted to 1% for 1.5 hour at room temperature. Another 13,000 RPM centrifuge was done before the Micro BCA assay.

To test the collagenase activity, liposomal collagenase after dialysis or free collagenase in phosphate buffered saline at a concentration of 5 ug/ml, were incubated at 37°C. Every hour, a collagenase sample was assessed for its capacity to cleave a fluorescein conjugated gelatin substrate (Thermo Fisher). Activity of the released collagenase was determined in accordance to the change in fluorescence over 3 minutes, relative to the fluorescence at t=0.

Stress/strength profile of collagen fibers exposed to collagenase

Collagen type I bundles, sourced from the tails of Wistar rats[25], were suspended using a LLOYD LF-Plus Digital Material Tester force machine. The bundles were suspended inside a bath loaded with a buffer that simulates the composition of the oral fluid: an isotonic solution, pH 6.7 at 37 oC complemented with electrolytes including sodium, potassium, calcium, magnesium, bicarbonate, and phosphates[26]. The bundles, 0.8-1.2 mm in diameter, were cut into two equal 4-cm sections, acting as an internal control. Collagenase type I from Clostridium histolyticum (Sigma-Aldrich) was added at different concentrations and the stress/strength profile of the collagen fibers was recorded as a function of the collagenase treatment. The Ultimate Tensile Strength (UTS) of the collagen bundle was determined for each collagenase concentration.

Fibroblasts adherence to collagen fibers

The fibroblast's morphological change was recorded using The LSM 710 -laser scanning confocal microscope (Zeiss) over a period of 90 minutes. The fibroblasts nuclei were stained using Hoechst 33342 (Thermo Fisher Scientific, MA, USA). The Hoechast 16.23 mM stock solution was diluted 1:2000 in Dulbecco's Phosphate Buffer Saline (DPBS, Sigma-Aldrich, St. Louis, USA) and the collagen fiber buffer was removed. 3 µl of the diluted solution was added, followed by 10 minutes light protected incubation. The staining solution was removed, and the fiber was washed 3 times in PBS.

Movie. S1. of the fibroblasts morphological change can be seen at: https://youtu.be/4krwecUS7Yc

Collagen regeneration SEM

In order to prepare the high-resolution scanning electron microscopy (HR-SEM) samples (Zeiss Ultra plus), we placed the bundles on a carbon fiber stab tape and dried them in a closed sample box. The bundles were observed using the Everhart-Thornley secondary electron detector. Each bundle was then cut in half. The untreated half acted as an internal control for each treated bundle. All presented data points are the mean of 14-20 experimental points. In order to weaken the bundles, collagen fibers were exposed to 0.05 mg/ml collagenase for 8 hours. Ethylenediaminetetraacetic acid (EDTA; ST. Louis, USA) in final concentration of 3mM along with two drops of NH_4Cl 1M buffer were added for 30

minutes in order to inhibit the enzyme's activity. Subsequently, the media was removed, and the treated bundles were washed two times with new growth media to allow bundle regeneration.

Collagen fibers regain their initial mechanical strength post nano-surgery

Collagen fibers were sourced from tails of Wistar rats. Each bundle was cut in half. The untreated half acted as an internal control for each treated bundle. All presented data points are the mean of 14-20 experimental points. Collagen fibers were exposed to collagenase at concentration of 0.05 mg/ml for 8 hours in order to weaken the bundles. After 8 hours a concentration of 0.02M ethylene diamine-tetra-acetic acid (EDTA; ST. Louis, USA) was added for 15 min in order to inhibit the enzyme activity hence allowing the bundle regeneration. Subsequently, the media was removed, and the treated bundles were washed twice with new growth media.

RNA extraction, PCR and RT-PCR

mRNA was extracted from the rats' gingival tissue using a TRIzol reagent **(**Thermo Fisher Scientific, MA, USA). The mRNA sequences were first reverse-transcribed to complementary DNA (cDNA) with reverse transcriptase using a thermocycler (LabCycler SensoQuest PCR, SensoQuest, Germany). To quantify the genes real time-PCR was employed (BioRad CFX96, Bio-Rad Laboratories Ltd., Israel). Each gene was independently amplified using specific probe and primers. Cycling times: 5 min at 95 °C, (15 sec at 95 °C, 45 sec at 63°C) X40 cycles.

Tooth displacement model

All animal trials followed the Technion Institutional Ethical Committee's guidance. All rats were anesthetized in two stages. In the first stage the rats were anesthetized with isoflurane. In the second stage each rat was injected intraperitoneal with a mixture of Ketamine and Xylazine. After each procedure, the rats were transferred and kept in an incubator, with constant oxygen flow, until they reached full recovery.

An ordinary orthodontic Ni-Ti closed coil spring (9 mm closed coil spring nickel and titanium alloy that has 2 eyelets with an inner radius of 0.76 mm) was used to connect the 1st molar in the upper pallet to the front upper incisors of the rat. The Ni-Ti coil spring was glued to the tooth (3M UNITEK), which generates constant force of 200 grams (1.96 N) when extended between 12-24 mm. The force applied in the oral cavity was the same on all the rats that participated in the experiment. This type of coil has been used and studied in orthodontics for years and has proven to be effective in orthodontic procedures. The procedure of installing the Ni-Ti coil closed spring was performed using human orthodontics equipment and materials. The 1st upper molar and the upper incisors were dried and cleaned using cotton swabs to remove any debris that accumulates. The teeth were conditioned using Transbond Plus etching primer conditioning agent by 3M UNITEK for 5-10 seconds creating a rugged surface to allow for stronger bonding. Following the conditioning, a small amount of composite Transbond LR light-cure adhesive (3M UNITEK) was spread over the molar. The eyelet ring of the Ni-Ti closed coil spring was placed in parallel with the tooth and light cured using LEDEX dental curing light for 10-15 seconds. Once again, a small

amount of bonding agent was spread over the ring and light cured for at least 40 seconds. The binding of the incisors was performed in a similar manner. Cleaning, drying and conditioning of the incisors were initially done. Subsequently, a stainless ligature was placed through the second eyelet ring of the Ni-Ti closed coil spring and we were able to achieve strong binding by braiding it around the incisors.

Collagenase-liposomes (see above Liposome Preparation), or a similar concentration of free collagenase, were applied directly to the sulcus. To apply the formulations a 30G needle was inserted carefully into the sulcus pocket, in a downward motion that was parallel to the tooth to a depth of ~1-2 mm, and a 50 μl volume was deposited to the buccal and lingual side of the tooth. The total duration of the studies was 60 days: 15 days of braces with the different treatments and an additional 45 days of recovery (after the braces removal). During the 15 days of treatment tooth displacement measurements were taken every 3 days using a digital caliper with an instrument error of 0.02 mm and microCT scans were performed on day 15 and day 60. The distance between the eyelet of the Ni-Ti closed coil on the first molar and the back of the upper incisors was measured and recorded using the digital caliper. Before each tooth displacement measurement, the rats were weighed and then anesthetized using isoflurane. This kind of anesthesia allowed fast measurements and short recovery time for the rats.

Histology

After sacrificing the rats, the entire maxilla was extracted and kept in 10% Natural Buffer Formalin (NBF) at room temperature. Paraffin-embedded tumor blocks from the rat maxillas were prepared and sectioned in 4μm-thick slides and stained with hematoxylin-eosin (H&E). Axial and sagittal cuts from the upper jaw were observed.

CT scans

The rats were euthanized and scanned using the Skyscan Micro CT (Bruker, UK) with 32-micron resolution definition. The scan was done using the following parameters: source voltage of 70 kV, source current of 355uA, exposure of 90 ms and rotation step of 0.8 deg. The scan reconstructions were performed using an NRecon program version 1.6.9.8.

Statistical analysis

Data is presented as means ±SD. Graphs. All statistical comparisons were performed with a two-tailed *t*-test for independent samples. P-value of <0.05 was considered to denote statistical significance. Singular factor ANOVA analysis was used among the tooth movement and the gene expression experiments to determine significantly difference.

Supplementary Material

Refer to Web version on PubMed Central for supplementary material.

Acknowledgments

This study was supported by ERC-STG-2015-680242.

Europe PMC Funders Author Manuscripts

The authors also acknowledge the Israel Ministry of Economy for a Kamin Grant (52752); the Israel Ministry of Science Technology and Space – Office of the Chief Scientist (3-11878); Israel Science Foundation (1778/13); Israel Cancer Association (2015-0116); German-Israeli Foundation for Scientific Research and Development for a GIF Young grant (I-2328-1139.10/2012); European Union FP-7 IRG Program for a Career Integration Grant (908049); a Mallat Family Foundation Grant; Alon and Taub Fellowships to A.S. Dr. Nitsan Dahan and Mrs Yehudith Schmidet for their help during the scanning confocal and electron microscopy; Dr. Oscar Lichtenstein for his help with the ex-vivo collagen stressing tests; Dr. R. Shofty, Dr. D. Levin-Ashkenazi, Ms. V. Zlobin, Mr. N. Amit from the Technion Pre-Clinical Research Authority for their help with the in-vivo animal tests, Ms. Bonnie Manor, Mr. Guy Nawi, Mr. Dima Zagorski and Mr. Rohan Aggarwal for graphical aid. Ms Shirley Pattisson for editing the manuscript. Merkel Technologies for their support in performing micro-CT scans on the BrukerCT/ Skyscan 1176.

References

1. Brown JL, Nash KD. The Economics of Orthodontics. American Association of Orthodontists Report. 2015
2. Nakashima M, Reddi AH. The application of bone morphogenetic proteins to dental tissue engineering. Nat Biotechnol. 2003; 21(9):1025–32. [PubMed: 12949568]
3. Vollenweider M, Brunner TJ, Knecht S, Grass RN, Zehnder M, Imfeld T, Stark WJ. Remineralization of human dentin using ultrafine bioactive glass particles. Acta Biomater. 2007; 3(6):936–43. [PubMed: 17560183]
4. Fernandez-Moure JS, Evangelopoulos M, Colvill K, Van Eps JL, Tasciotti E. Nanoantibiotics: a new paradigm for the treatment of surgical infection. Nanomedicine. 2017; (0)
5. Vishwakarma A, Bhise NS, Evangelista MB, Rouwkema J, Dokmeci MR, Ghaemmaghami AM, Vrana NE, Khademhosseini A. Engineering Immunomodulatory Biomaterials To Tune the Inflammatory Response. Trends in biotechnology. 2016; 34(6):470–82. [PubMed: 27138899]
6. Solomonov I, Zehorai E, Talmi-Frank D, Wolf SG, Shainskaya A, Zhuravlev A, Kartvelishvily E, Visse R, Levin Y, Kampf N, Jaitin DA, et al. Distinct biological events generated by ECM proteolysis by two homologous collagenases. Proceedings of the National Academy of Sciences. 2016; 113(39):10884–10889.
7. Ghadiali JE, Stevens MM. Enzyme-responsive nanoparticle systems. Advanced Materials. 2008; 20(22):4359–4363.
8. Gilpin D, Coleman S, Hall S, Houston A, Karrasch J, Jones N. Injectable collagenase Clostridium histolyticum: a new nonsurgical treatment for Dupuytren's disease. The Journal of hand surgery. 2010; 35(12):2027–2038. e1. [PubMed: 21134613]
9. Jang, HL, Zhang, YS, Khademhosseini, A. Boosting clinical translation of nanomedicine. Future Medicine; 2016.
10. Stark WJ. Nanoparticles in biological systems. Angew Chem Int Ed Engl. 2011; 50(6):1242–58. [PubMed: 21290491]
11. Shilo M, Berenstein P, Dreifuss T, Nash Y, Goldsmith G, Kazimirsky G, Motiei M, Frenkel D, Brodie C, Popovtzer R. Insulin-coated gold nanoparticles as a new concept for personalized and adjustable glucose regulation. Nanoscale. 2015; 7(48):20489–96. [PubMed: 26583784]
12. Hafner A, Lovric J, Lakos GP, Pepic I. Nanotherapeutics in the EU: an overview on current state and future directions. Int J Nanomedicine. 2014; 9:1005–23. [PubMed: 24600222]
13. Weissig V, Pettinger TK, Murdock N. Nanopharmaceuticals (part 1): products on the market. Int J Nanomedicine. 2014; 9:4357–73. [PubMed: 25258527]
14. Peer D, Karp JM, Hong S, Farokhzad OC, Margalit R, Langer R. Nanocarriers as an emerging platform for cancer therapy. Nat Nanotechnol. 2007; 2(12):751–60. [PubMed: 18654426]
15. Eliaz RE, Szoka FC Jr. Liposome-encapsulated doxorubicin targeted to CD44: a strategy to kill CD44-overexpressing tumor cells. Cancer research. 2001; 61(6):2592–601. [PubMed: 11289136]
16. Brown LR. Commercial challenges of protein drug delivery. Expert opinion on drug delivery. 2005; 2(1):29–42. [PubMed: 16296733]
17. Nagase H, Woessner JF. Matrix metalloproteinases. Journal of Biological Chemistry. 1999; 274(31):21491–21494. [PubMed: 10419448]

18. Wilson JJ, Matsushita O, Okabe A, Sakon J. A bacterial collagen-binding domain with novel calcium-binding motif controls domain orientation. The EMBO Journal. 2003; 22(8):1743–1752. [PubMed: 12682007]
19. Reznikov N, Steele JAM, Fratzl P, Stevens MM. A materials science vision of extracellular matrix mineralization. Nature Reviews Materials. 2016; 1
20. Mwenifumbo S, Stevens MM. ECM interactions with cells from the macro-to nanoscale. Biomedical Nanostructures. 1:225–260.
21. Harris AK, Stopak D, Wild P. Fibroblast traction as a mechanism for collagen morphogenesis. Nature. 1981; 290(5803):249–51. [PubMed: 7207616]
22. Molinaro R, Corbo C, Martinez JO, Taraballi F, Evangelopoulos M, Minardi S, Yazdi IK, Zhao P, De Rosa E, Sherman MB, De Vita A, et al. Biomimetic proteolipid vesicles for targeting inflamed tissues. Nat Mater. 2016; 15(9):1037–1046. [PubMed: 27213956]
23. Johnston CD, Littlewood SJ. Retention in orthodontics. Br Dent J. 2015; 218(3):119–22. [PubMed: 25686428]
24. Brinckerhoff CE, Plucinska IM, Sheldon LA, O'Connor GT. Half-life of synovial cell collagenase mRNA is modulated by phorbol myristate acetate but not by all-trans-retinoic acid or dexamethasone. Biochemistry. 1986; 25(21):6378–84. [PubMed: 3024708]
25. Rajan N, Habermehl J, Coté M-F, Doillon CJ, Mantovani D. Preparation of ready-to-use, storable and reconstituted type I collagen from rat tail tendon for tissue engineering applications. Nature protocols. 2007; 1(6):2753–2758.
26. Humphrey SP, Williamson RT. A review of saliva: Normal composition, flow, and function. The Journal of Prosthetic Dentistry. 2001; 85(2):162–169. [PubMed: 11208206]

Europe PMC Funders Author Manuscripts

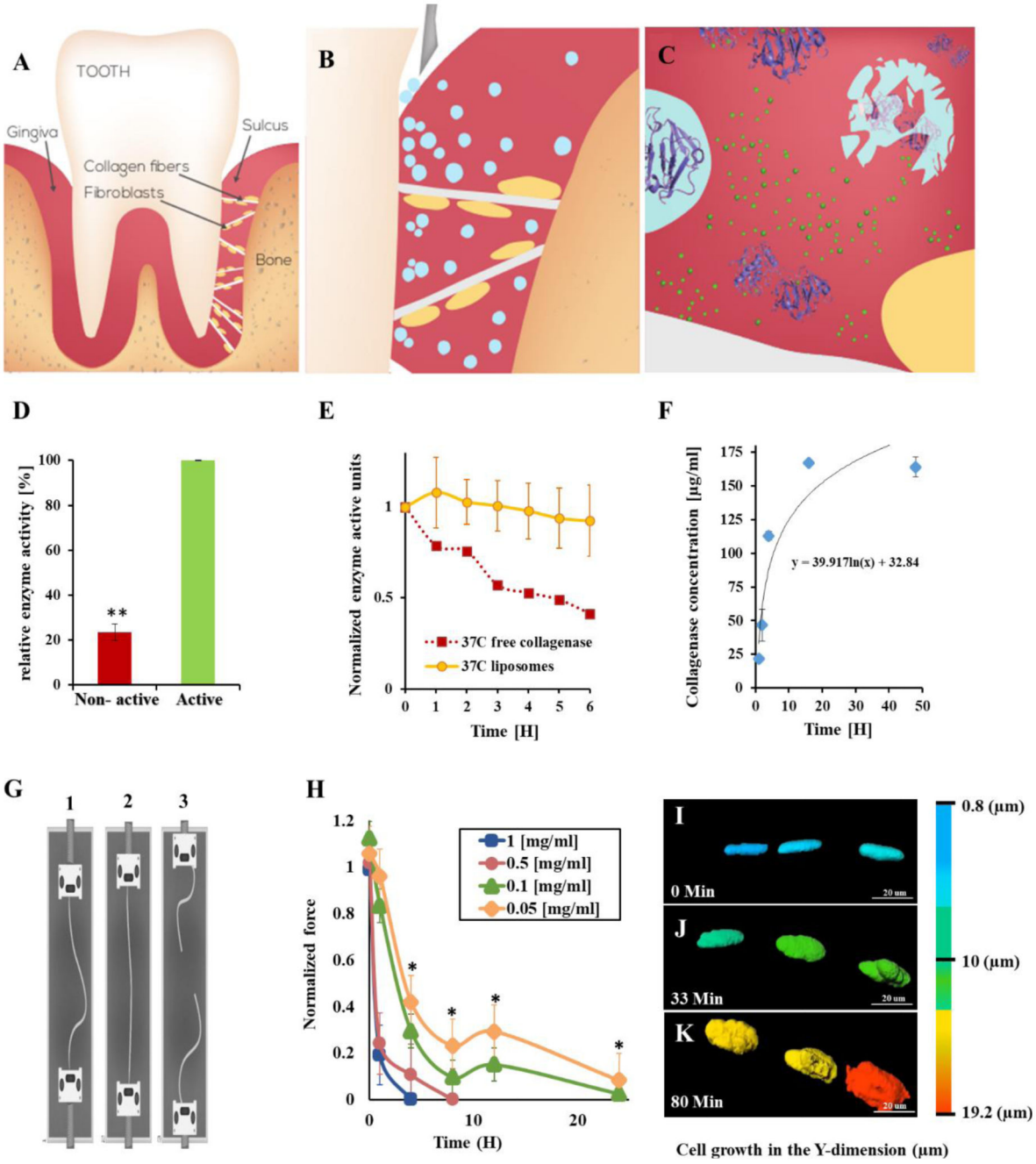

Figure 1. Nanosurgery – enzymes loaded into nanoparticles are released at the surgical site, where they are activated, to perform a localized surgical task.

Proteolytic enzymes, housed within nanoparticles replace the traditional blade, thereby, cutting only the target tissue, reducing pain and enhancing recovery. We utilized this approach to replace a surgical procedure in the oral tissue. Teeth are confined to their natural orientation by soft and hard tissue (A). Specifically, collagen type-1 fibers anchor the teeth to the underlying bone. Nanoparticles (blue spheres) loaded with collagenase, a proteolytic enzyme with specificity towards collagen, are inserted into the sulcus (B). The particles house the enzyme in a deactivated form. Once released, the Ca^{+2} naturally present in the

tissue activates the enzyme and collagen degradation begins. The nanoparticles maintain the enzyme's therapeutic release profile and confine the biodistribution to the treatment site. (C) This facilitates enhanced orthodontic tooth movement. The collagen fibers recover rapidly after the treatment.

Controlled release and activation. Collagenase released from the nanoparticles over 48 hours at physiological conditions (F). Once released, the enzyme is activated by its cofactor calcium, naturally present in the tissue (D). The activity of the collagenase declines thereafter, over a period of 6 hours (E). As long as the enzyme is housed inside the particle it remains protected and inactive (D, and Supplementary Fig. S7A,B).

Collagenase relaxes collagen fibers. Collagen fibers were exposed to collagenase at various concentrations for different periods of time. The fibers were stressed using a force machine under oral physiological conditions (G, Supplementary Fig. S2, S7C). As the collagenase concentration increased, the fibers weakened (H). The higher collagenase concentrations (0.5 and 1 mg/mL) degraded the collagen fibers within less than 10 hours. A therapeutic window of 0.05 - 0.1 mg/ml at which the collagen fibers were relaxed but not fully degraded by collagenase was determined.

Fibroblast morphology changes as a function of collagenase activity. A collagen fiber (beneath the optical field) with adherent fibroblasts in focus was imaged during the process of collagenase treatment. As the collagen fiber relaxes, the adherent fibroblasts change their morphology from an elongated structure to a round structure (I→J→K, collagenase was added at t=0). A full time-lapse movie of the process is presented at: https://youtu.be/4krwecUS7Yc. It is important to note that the collagenase relaxed the collagen fibers but did not detach the fibroblasts nor impact their viability.

Error bars indicate the standard deviation of at least five independent measurements. ** indicates two tail P-Value <0.01.

Europe PMC Funders Author Manuscripts

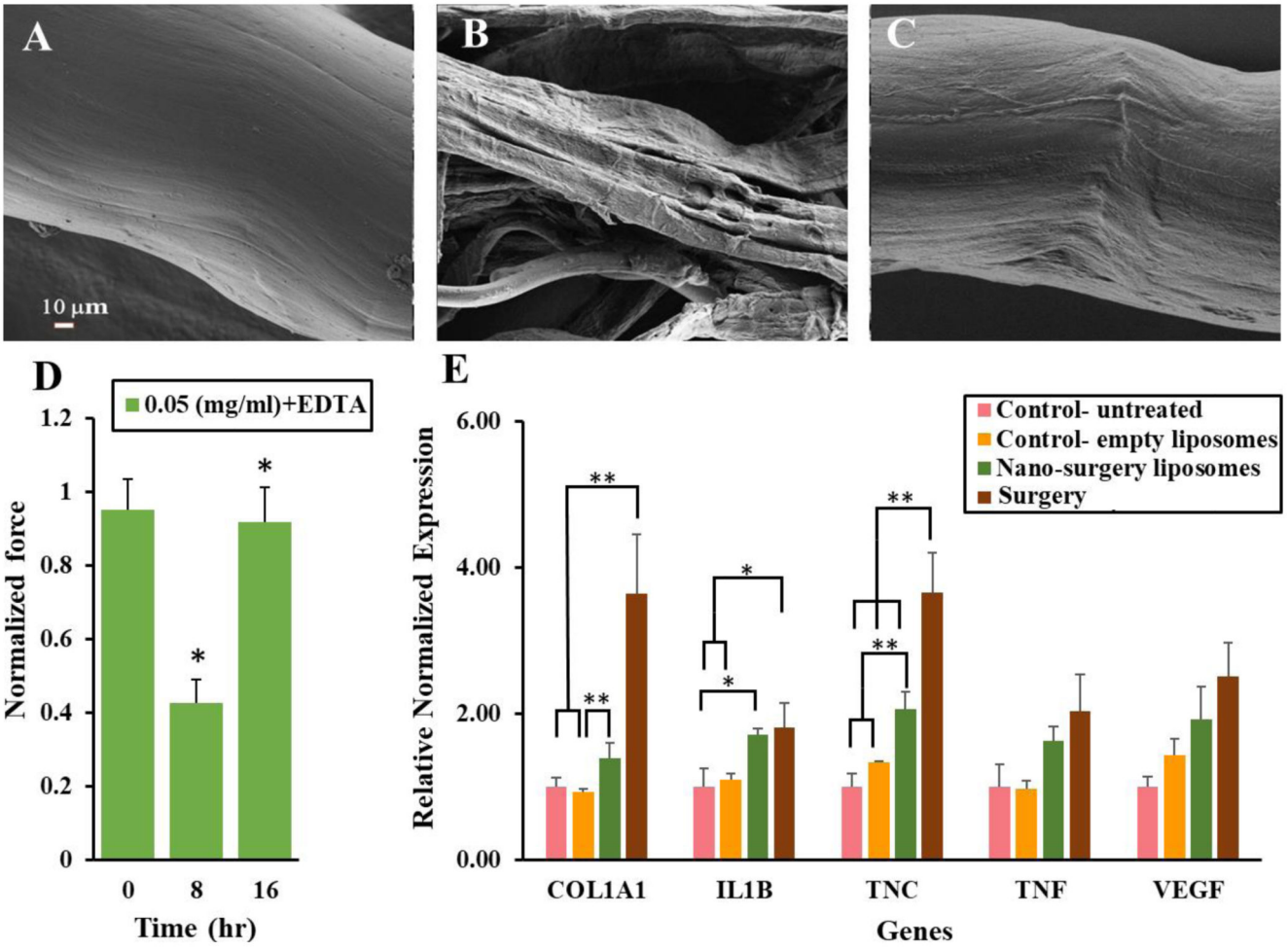

Figure 2. Collagen regeneration.

A collagen fiber was imaged using HR-SEM before (A) during (B) and after being exposed to collagenase, allowing collagen regeneration (C).

Collagen relaxation and regeneration. Collagen fibers were stressed using a force machine. Strength measurements were performed before adding the collagenase, during the collagenase disassembling activity, and 16 hr after the collagenase activity was retarded. The collagen fibers regained ~90% of their initial strength profile (D).

All data points are the mean of 14-20 experiments.

Regenerative genes are upregulated at the treatment site. Collagenase type-1 was inserted into rat's sulcus, *in vivo*. Twenty-four hours later, the tissue surrounding the teeth was collected and RNA was isolated (E). The RNA profile of Col1A1, IL1b, TNC, VEGF and TNFα (genes associated with collagen repair and extracellular matrix remodeling) was measured. β-2 microglobulin (B2M) was used as the relative housekeeping gene. *indicates a two tail, unequal variances P-Value <0.05,** indicates a two tail unequal variances P-Value <0.01, singular factor ANOVA analysis confirmed significant difference between the means.

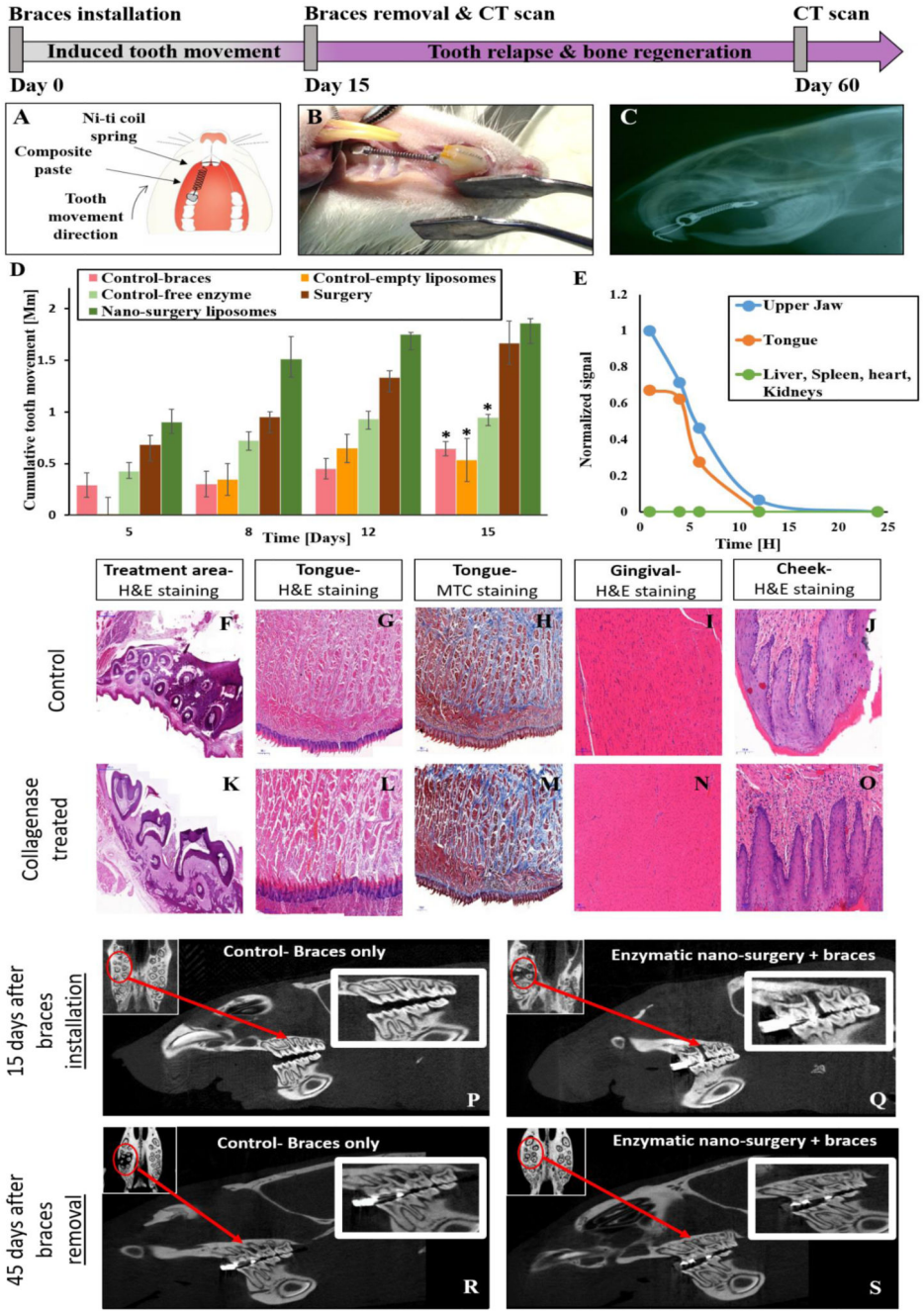

Figure 3. Accelerating orthodontic treatments with a local application of enzymes.

Nanoparticles containing a therapeutic dose of collagenase (0.2 mg/ml) were inserted into the sulcus of Wistar rats. An orthodontic spring was used to connect the front upper right molar to the incisors, generating a constant pull force of 2N (A – schematic, B – photograph). A lateral X-ray scan of a Wistar rat with an orthodontic spring connecting the front upper right molar to the incisors generated a constant pull force of 2N (C). The gap between the front incisors and molar was measured over time using a caliper and the effect of the procedure on the underlying tissue was evaluated.

Europe PMC Funders Author Manuscripts

Tooth displacement was measured over a period of 15 days with and without nano-surgery or in comparison to oral surgery. Three test groups consisted of rats treated with nanoscale liposomes, free enzyme or oral surgery. Two control groups consisted of rats with braces only or a sham treatment with empty liposomes (D). *indicates a two tail, unequal variances P-Value <0.05 compared to the nano-surgery liposomes group, singular factor ANOVA analysis confirmed significant difference between the means.

Liposome biodistribution. The biodistribution of nano-liposomes was tracked. Organs were collected at different time points with the highest florescent levels measured at the treatment site (E). After 4 hours a 50% decrease in the signal was recorded. After approximately 12 hours the signal was below detection (Supplementary Fig. S9).

Histological evaluation of collagenase-treated tissues. Seven days after placing the collagenase-liposomes in the rat sulcus, oral tissues of the control (G-J) and treated (L-O) groups were stained with H&E and Masson's trichrome. Both histological groups appear similar, specifically, no difference was noticed between the control to the treated group after 15 days of treatment surrounding the treatment area (F,K).

Bone regeneration after nano-surgery. Hard and soft tissue regeneration is imperative for surgical recovery. We compared bone regeneration with and without the enzymatic nano-surgery. Liposomal collagenase was placed in the rat's upper right molar sulcus together with an orthodontic spring, among the test group for 15 days. Lateral and axial views of the control (braces only) (P) and nano-surgery (Q) groups were imaged by microCT on day 15. The tooth enhanced movement can be noticed between the front and second molars and is marked with red circles and arrows. Full bone regeneration was observed 60 days after initiating the treatment (45 days after removing the braces) in the nano-surgery group (S), but not in the normal orthodontic group (R).

Europe PMC Funders Author Manuscripts